View metadata, citation and similar papers at core.ac.uk
brought to you by CORE
provided by University of Lincoln Institutional Repository

DE G

Fractional Calculus & Applied Analysis
An International Journal for Theory and Applications
VOLUME 20, NUMBER 3 (2017)
(Print) ISSN 1311-0454
(Electronic) ISSN 1314-2224

RESEARCH PAPER

IMPACT OF FRACTIONAL ORDER METHODS ON OPTIMIZED TILT CONTROL FOR RAIL VEHICLES

Fazilah Hassan [1], **Argyrios Zolotas** [2]

Abstract

Advances in the use of fractional order calculus in control theory increasingly make their way into control applications such as in the process industry, electrical machines, mechatronics/robotics, albeit at a slower rate into control applications in automotive and railway systems. We present work on advances in high-speed rail vehicle tilt control design enabled by use of fractional order methods. Analytical problems in rail tilt control still exist especially on simplified tilt using non-precedent sensor information (rather than use of the more complex precedence (or preview) schemes). Challenges arise due to suspension dynamic interactions (due to strong coupling between roll and lateral dynamic modes) and the sensor measurement. We explore optimized PID-based non-precedent tilt control via both direct fractional-order PID design and via fractional-order based loop shaping that reduces effect of lags in the design model. The impact of fractional order design methods on tilt performance (track curve following vs ride quality) trade off is particularly emphasized. Simulation results illustrate superior benefit by utilizing fractional order-based tilt control design.

MSC 2010: Primary 26A33; Secondary 34A08, 70Q05, 93B52, 93C35, 93C95, 37N35

Key Words and Phrases: fractional order control; optimization; tilt control; non-minimum phase zeros; railway vehicles; active suspensions

© 2017 Diogenes Co., Sofia
pp. xxx–xxx , DOI: 10.1515/fca-2017-.....

1. **Introduction**

Tilting is a quite successful concept of high-speed trains that offers a solution to "make rail vehicles run faster hence reduce journey times" on railway routes without the need of substantial change on infrastructure. The idea is straightforward and based on the cycle/motorcycle rider trick of "lean in towards the curve to go faster and feel more comfortable". Similarly, tilting trains lean in towards the railtrack corner (via tilt mechanism) to reduce passenger lateral acceleration and enable increased vehicle speed. Tilting train technology was highlighted in the 2014 article of BBC future [19] on the new ZEFIRO tilting train. In addition, tilting trains continue evolving in terms of their structure and tilt mechanisms [7] that facilitates further exploration of advanced control design.

Most tilting trains nowadays use the command-driven with precedence tilt control approach devised in the early 1980s as part of the UK-led Advanced Passenger Train development [4]. Precedence (or preview) schemes use signals from the vehicle in front to provide preview information, carefully designed so that the delay introduced by the filtering during communication compensates for the preview time. There has been some further developments of the concept, i.e. use of GPS database and/or additional sensors, but the overall principles essentially remain the same. It is worth noting that achieving a satisfactory local/vehicle tilt control scheme is still an important research question due to facilitating system simplifications and more straightforward fault detection.

Concentrating on the tilt control approach, a number of studies exist [24] [38] (and references within) [37]. Albeit no study exists on an in-depth investigation of fractional order control for the tilt problem. Without doubt fractional order calculus [14] has an immense impact on enhancing control theory and design of simpler controller structures for complex applications. In fact, Fractional order (FO) systems have received substantial attention in the last two decades, with a number of modelling approaches and control design techniques developed. In particular, there is a large number of papers in fractional PID control design as well as control design via loop shaping. A number of references exist in the literature with few suggested here (and references within), e.g. [23], [28], [29], [27], [33], [2], [15].

This paper contributes to the impact fractional order calculus, through the channel of fractional order control, has in the area of high speed railway vehicles, i.e. advanced tilt control design. The paper's contribution strongly aligns with a viewpoint highlighted in [14], i.e. quoting Y.-Q. Chen, *the "Need to show that fractional calculus enables better performance (result) than the best achievable ones previously using integer-order calculus"*.

The paper is organized as follows: Section 2 introduces the vehicle model including an insight into non-minimum phase characteristics. Section 3 presents the design setup and a brief introduction to the assessment process. Design of conventional integer-order PID control is followed in Section 4 including performance limitations. Section 5 introduces fractional order methods and follows a rigorous design of fractional order based controllers from both a direct FOPID design and via loop-shaping approach with non-minimum phase cancellation shaping. In the same section, controller order reduction is emphasized as a means of easier implementation. Section 6 presents simulation and related analysis emphasizing robustness properties. Finally, conclusions are drawn in Section 7.

2. **Modelling and system dynamics**

2.1. **Endview diagram.** The model is based on the end-view of a typical tilt across secondary (with anti-roll bar- referred to as ARB) train vehicle, see Figure 1. The mathematical representation of the tilt model is shown in [39], including detailed discussion on the modelling parameters and variables.

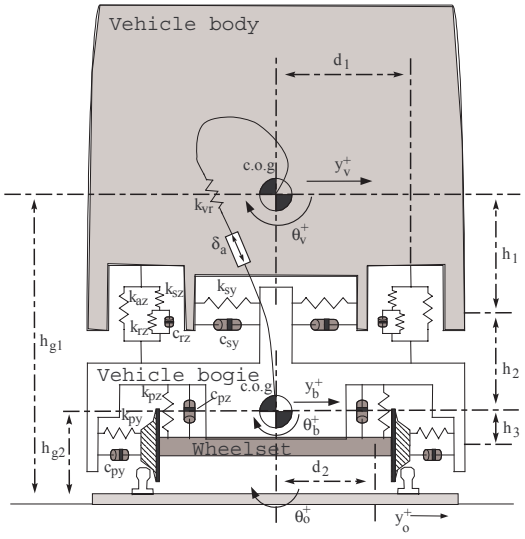

FIGURE 1. Vehicle end-view

The overall roll angle from the horizon (track elevation + expected tilt) is not to exceed ≈ 14 degrees which supports the use of a linearized model for robust control design. From the vehicle equations, a (nominal) design model transfer function (TF), $G_{yu}(s)$ is given by (2.1). This represents

the dynamic relationship between effective cant deficiency $Y_{(e.c.d)}$ (for 60% tilt compensation) and the control input $\Delta_{(t-i)}$ (ideal control tilt angle). In fact, the effective cant deficiency is the indicator on how much tilting requires to provide the reduction in passenger acceleration at higher speed.

$$G_{yu}(s) = \frac{27531(s+26.18)(s+40.73)}{(s+23.2)(s^2+1.38s+17.44)(s^2+5.11s+88)} \cdots \frac{(\mathbf{s-29.36})(\mathbf{s-6.02})}{(s^2+22s+483.6)(s^2+29.15s+4888)} \cdots \frac{(s^2+7.65s+24.44)}{(s^2+4.825s+15870)(s^2+41.73s+28440)}. \tag{2.1}$$

This is a 13th order plant TF utilized for tilt control design (after minimal realization), and highlighted is the nominal location of the NMP zeros.

2.2. **Insight into the Non Minimum Phase model characteristic.** The nature of the NMP zeros of the SISO TF is due to the location of the suspension -relative to the centre of gravity of the vehicle body (cog) and the centre of tilt- and the roll angle contribution (from portion of the gravitational force) measured by the lateral accelerometer. Symbolic analysis is meaningful on a simpler (physically reduced) 4th order model with no air-spring. This result is approximate as it includes only the secondary suspension dynamics (while disregarding bogie, airpring and kinematics contribution). However, the validity of the analysis stands as the neglected modes do not largely affect the NMP zeros location. The 4th order model symbolic state space matrices (state, control and output respectively) are:

$$A_2 = \begin{bmatrix} 0 & 0 & 1 & 0 \\ 0 & 0 & 0 & 1 \\ -\frac{2\,k_{\mathrm{sy}}}{m_{\mathrm{v}}} & \frac{2\,h_1\,k_{\mathrm{sy}}}{m_{\mathrm{v}}} & -\frac{2\,c_{\mathrm{sy}}}{m_{\mathrm{v}}} & \frac{2\,c_{\mathrm{sy}}\,h_1}{m_{\mathrm{v}}} \\ \frac{2\,h_1\,k_{\mathrm{sy}}+g\,m_{\mathrm{v}}}{i_{\mathrm{vr}}} & -\frac{2\,k_{\mathrm{sy}}\,{h_1}^2+k_{\mathrm{vr}}}{i_{\mathrm{vr}}} & \frac{2\,c_{\mathrm{sy}}\,h_1}{i_{\mathrm{vr}}} & -\frac{2\,c_{\mathrm{sy}}\,h_1^2}{i_{\mathrm{vr}}} \end{bmatrix}, \tag{2.2}$$

$$B_2 = \begin{bmatrix} 0 & 0 & 0 & \frac{k_{\mathrm{vr}}}{i_{\mathrm{vr}}} \end{bmatrix}^T, \tag{2.3}$$

$$C_2 = \begin{bmatrix} \frac{6\,k_{sy}}{5\,g\,m_{\mathrm{v}}} & -\frac{6\,h_1\,k_{sy}-5\,g\,m_{\mathrm{v}}}{5\,g\,m_{\mathrm{v}}} & \frac{6\,c_{sy}}{5\,g\,m_{\mathrm{v}}} & -\frac{6\,c_{sy}\,h_1}{5\,g\,m_{\mathrm{v}}} \end{bmatrix}. \tag{2.4}$$

We use state space here to illustrate transmission zeros. The state vector includes $\left[y_{\mathrm{v}}, \theta_{\mathrm{v}}, \dot{y}_{\mathrm{v}}, \dot{\theta}_{\mathrm{v}}\right]$ (i.e. body: lateral, roll, lateral rate, roll rate, resp.). The output matrix C_2 refers to the effective cant deficiency for 60% tilt compensation on steady-state curve.

DEFINITION 2.1. For a system Σ_p represented in state space by the triple $\{A, B, C\}$, its invariant zeros are the values of $s \in \mathbb{C}$ such that its *Rosenbrock matrix*, $RSM(s) = \begin{bmatrix} sI - A & -B \\ C & 0 \end{bmatrix}$, looses normal rank.

For a minimal state space realization invariant and transmission zeros coincide. From a practical point of view, the system zeros refer to the case of a zero output for some non-zero input acting on the system. In fact, the zeros are the solution of $\det(RSM(s)) = 0$.

Given the simplified 4-state model, the determinant of the above $RSM(s)$ system matrix results to (a) a cubic polynomial in s if damping is $c_{\mathrm{sy}} \neq 0$; (b) a quadratic polynomial in s if damping is $c_{\mathrm{sy}} = 0$.

For case $c_{\mathrm{sy}} \neq 0$ the characteristics of the system give negative cubic discriminant, and its roots comprise a real root and a complex pair. The real root is positive (reflecting the location of the slow NMP zero) and, after tedious calculations (and extended symbolic analysis), given by

$$\begin{aligned} z_p = & \dots \\ & \dots + \sqrt[3]{\sqrt{r_{fc}} - \frac{\left(\frac{k_{\mathrm{sy}}}{c_{\mathrm{sy}}} - \frac{5\,g\,m_{\mathrm{v}}}{6\,c_{\mathrm{sy}}\,h_1}\right)^3}{27} - \frac{5\,g\,\left(\frac{9\,k_{\mathrm{sy}}}{c_{\mathrm{sy}}} - \frac{15\,g\,m_{\mathrm{v}}}{2\,c_{\mathrm{sy}}\,h_1}\right)}{162\,h_1} + \frac{5\,g\,k_{\mathrm{sy}}}{6\,c_{\mathrm{sy}}\,h_1}} \\ & \dots + \sqrt[3]{-\sqrt{r_{fc}} - \frac{5\,g\,\left(\frac{9\,k_{\mathrm{sy}}}{c_{\mathrm{sy}}} - \frac{15\,g\,m_{\mathrm{v}}}{2\,c_{\mathrm{sy}}\,h_1}\right)}{162\,h_1} - \frac{\left(\frac{k_{\mathrm{sy}}}{c_{\mathrm{sy}}} - \frac{5\,g\,m_{\mathrm{v}}}{6\,c_{\mathrm{sy}}\,h_1}\right)^3}{27} + \frac{5\,g\,k_{\mathrm{sy}}}{6\,c_{\mathrm{sy}}\,h_1}} + \\ & \dots + \frac{5\,g\,m_{\mathrm{v}}}{18\,c_{\mathrm{sy}}\,h_1} - \frac{k_{\mathrm{sy}}}{3\,c_{\mathrm{sy}}}, \end{aligned} \tag{2.5}$$

with

$$\begin{aligned} r_{fc} = & \frac{\left(\frac{2\left(\frac{k_{\mathrm{sy}}}{c_{\mathrm{sy}}} - \frac{5\,g\,m_{\mathrm{v}}}{6\,c_{\mathrm{sy}}\,h_1}\right)^3}{27} + \frac{5\,g\left(\frac{9\,k_{\mathrm{sy}}}{c_{\mathrm{sy}}} - \frac{15\,g\,m_{\mathrm{v}}}{2\,c_{\mathrm{sy}}\,h_1}\right)}{81\,h_1} - \frac{5\,g\,k_{\mathrm{sy}}}{3\,c_{\mathrm{sy}}\,h_1}\right)^2}{4} \dots \\ & - \frac{\left(\frac{\left(\frac{k_{\mathrm{sy}}}{c_{\mathrm{sy}}} - \frac{5\,g\,m_{\mathrm{v}}}{6\,c_{\mathrm{sy}}\,h_1}\right)^2}{3} + \frac{5\,g}{3\,h_1}\right)^3}{27}, \end{aligned} \tag{2.6}$$

note that finding the complex pair of roots is not necessary as, for the tilt system, these naturally reflect the stable complex zero location.

For the case $c_{\mathrm{sy}} = 0$ the state matrix is largely simplified (as all contributions of c_{sy} are now neglected) and the result greatly simplifies to a set of real roots. The positive root relates to the aforementioned NMP zero,

i.e.

$$z_p|_{(c_{\rm sy}=0)} = \sqrt{\frac{10\,g\,k_{\rm sy}}{6\,h_1\,k_{\rm sy} - 5\,g\,m_{\rm v}}}.$$

The contribution of the suspension location and lateral-roll dynamic coupling can be clearly seen.

We also provide the numerical values for the location of the slower NMP zero (which is the most important one in limiting closed-loop bandwidth for all the three models, i.e. $z_p|_{(c_{\rm sy}=0)} \approx 7.35$ (4-state model, no damping); $z_p|_{(c_{\rm sy}\neq 0)} \approx 5.47$ (4-state model, with damping); $z_p = 6.02$ (13th order model). Note that the simplified (approximate) 4th order model with damping reflects a slightly slower NMP zero location. The simplified model used here is only to illustrate the nature of the important NMP zero in the model (the one that mainly hinders fast tilt response).

2.3. **Exogenous inputs that excite the vehicle.** Regarding track inputs, $G_{yd}(s)$ is a matrix TF, i.e.

$$Y_{ecd}(s) = \mathbf{G}_{yd}(s) \left[\begin{array}{c} \mathbf{U_{t-det}}(s) \\ \mathrm{U_{t-sto}}(s) \end{array} \right],$$

where $\mathbf{U_{t-det}}(s)$ relates to intended rail track features (deterministic), and $\mathrm{U_{t-sto}}$ relates to the unintended (misalignment) track features (stochastic).

Track inputs (also used for simulation/assessment purposes) are: (i) a rail track corner with maximum cant angle $\theta_o^{\{\max\}} = 6$ deg, maximum curve radius $R_{\max} = 1$ km, transition length = 145 m at each end and track length = 1.2 km; (ii) the unintended track input was characterized by velocity spectrum [31]

$$\dot{S}_{\rm T}(f_{\rm t}) = \frac{(2\pi)^2 \Omega_{\rm l} v^2}{f_{\rm t}},\ (m/s)^2 (Hz)^{-1}, \tag{2.7}$$

noting that v is the vehicle speed (m/s) and $f_{\rm t}$ the temporal frequency. With $\Omega_l = 0.33 \cdot 10^{-8}$m (a typically medium-quality rail track) and tilting speed of 58 m/s.

For ride quality we assess the weighted lateral acceleration of passengers by W_Z Sperling index TF (for the index see [21]).

3. Design setup and brief introduction to tilt assessment

3.1. **Design setup.** The feedback structure for the controller designs is shown on Figure 2. We use a simplified setup, with no feed-forward of disturbances. The rationale is twofold: (i) accurate estimation of railtrack disturbance inputs is possible [40] but challenging, while adds complexity in the solution, (ii) the impact of fractional order methods on simple tilt control design is emphasized.

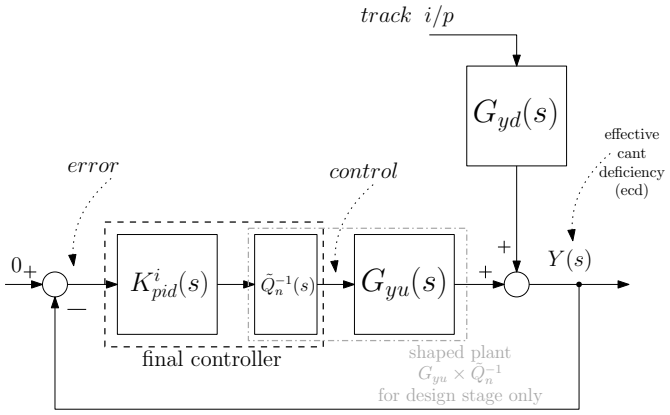

FIGURE 2. The feedback setup for the control designs (in the non-FO cases $\tilde{Q}_n^{-1} = 1$)

REMARK. A single figure is used to illustrate feedback control structure for designs, noting the following:
(a) For the integer order PID design (presented in this section) K^i_{pid} is an integer-order rational (IOR) TF and $Q_n^{-1} = 1$;
(b) For the fractional PID design (presented in section 5.2) K^i_{pid} is a fractional TF and $\tilde{Q}_n^{-1} = 1$;
(c) For the loop-shaping design (presented in section 5.3) K^i_{pid} is IOR TF and Q_n^{-1} is a fractional order shaping filter (although on the figure its rational order approximation is depicted, i.e. $\tilde{Q}_n^{-1}$). We refer to this approach as "loop-shaping" due to the way the filter is included to dictate partial cancellation of the NMP zero authority in the design.

Note that all PID controllers are implemented with derivative action cut-off frequency = 1000 rad/s (well above the frequency range of interest for the tilt system), i.e.

$$K_{PID}(s) = k_p \left(1 + \frac{1}{\tau_i s} + \frac{\tau_d s}{\frac{s}{N} + 1}\right), \tag{3.1}$$

where $k_p, \tau_i, \tau_d, N \in \mathbb{R}^+$ (proportional gain, integral time constant, derivative time constant, derivative cut-off freq., resp.)

With conventional PID being the most popular controller in industrial applications, a number of rules and design techniques have been developed and exist in the control literature see for example [1], [34].

3.2. **Tilt control assessment.** From a controller assessment point of view the procedure used in [39] follows a rigorous approach for accessing the deterministic tilt control performance. Essentially separates the curve transition response into two aspects: (i) investigation of the fundamental tilting response based upon the PCT factor; (ii) investigation of the transitional dynamic suspension effects via comparison to the *ideal tilting* response. The PCT factor specifies the percentage of passengers, on a tilting train, feeling uncomfortable on the curve transition (based on a comprehensive experimental/empirical study undertaken in the 1980s and now is a European standard). For more details the readers are referred to [39], [38].

4. Integer order PID control design

4.1. **Conventional PID design rules.** As discussed previously the SISO tilt control design transfer function is non-minimum phase. The simplest controller structure is a PID-type (integral to guarantee zero steady-state error on steady curve and proportional action to limit phase lag at high frequency). The conventional approach is to manually design via classical PID design rules (i.e. Ziegler-Nichols, Tyreus-Luyben etc.) or via frequency-response gain/phase margins and overall guaranteeing an acceptable performance level of tilt deterministic vs tilt stochastic trade-off. To illustrate the achieved performance by conventional integer-order PID, the following (typical in control design) approaches are utilized:

- Ziegler-Nichols (Z-N) on 1/4 decay ratio (original),
- Z-N de-tuned (with emphasized integral action),
- Tyreus-Luyben approach (mainly because it was based on the Z-N original but aims to less oscillatory response and reduced sensitivity in process conditions), Tyreus-Luyben detuned (to emphasize more integral action), and
- Frequency response design (F-R manual) providing GM approx. 5dB, PM approx. 45 deg, b/w approx. 1 rad/s. The manual designs are quite straightforward [1], [10], and hence we omit the details.

The controller gains for the manually designed PIDs are:

$$\begin{array}{rlll} \text{Z-N original:} & k_p = 0.6k_u, & \tau_i = 0.5T_u, & \tau_d = 0.125T_u \\ \text{Z-N detuned:} & k_p = 0.6k_u, & \tau_i = 0.25T_u, & \tau_d = 0.125T_u \\ \text{T-L original:} & k_p = k_u/2.2, & \tau_i = 2.2T_u, & \tau_d = T_u/6.3 \\ \text{T-L detuned:} & k_p = k_u/2.2, & \tau_i = 0.19T_u, & \tau_d = T_u/6.3 \\ \text{F-R manual:} & k_p = 0.1256, & \tau_i = 0.122, & \tau_d = 0.1829 \end{array}$$

where the ultimate gain (gain at which the closed-loop system is marginally stable) and period of such oscillations for the nominal TF are $k_u = 0.325$ and $T_u = 0.825$s, respectively.

The achievable (nominal) performance is shown on Table 1 (due to space limitations we do not present the detailed PCT related dynamic variables but only the PCT result) and Table 2. The F-R manual design offers improvement (but requires few design iterations to accomplish), still the achieved ride quality is slightly higher than the industrially accepted norm of 7.5% degradation. Clearly the NMP zero characteristic of the plant imposes hard bandwidth constraint [32], while achieving a low value for the module margin $\|S\|_\infty$ is a challenging task.

4.2. **Optimized integer-order PID control design.** Here the integer order PID is tuned via optimization, as follows

$$\begin{aligned} \underset{K_{pid}}{\text{minimize}} \quad & f(x) \\ \text{subject to} \quad & rqd \leq 7.5\% \\ & \|S(j\omega)\|_\infty \leq 2 \\ & \|W_\delta(j\omega)T(j\omega)\|_\infty \leq 1, \end{aligned} \tag{4.1}$$

where $f(x)$ is the PCT factor. The rationale behind this is to minimize the PCT factor (which combines dynamic variables relating to the deterministic performance), bounding the Module margin $\|S(j\omega)\|_\infty$ to allow for a degree of robustness [32], while imposing (stochastic) ride quality degradation allowance close to $\leq 7.5\%$ and guaranteeing robust stability to multiplicative uncertainty i.e. bounding $\|W_\delta(j\omega)T(j\omega)\|_\infty$ [10] (this will be explained in detail later in the robustness section, esp. the bound $W_\delta(j\omega)$).

The optimization runs over all integer order PID controllers and can be performed via nonlinear tools, e.g. Matlab's `fmincon()` (implementing the Nelder-Mead method), or via heuristics (i.e, GA). We employ `fmincon()` and a multi-start approach perturbing initial conditions (10 iterations with a random initial value generation in the interval $[0.01\vec{x}_0, 2\vec{x}_0]$ suffices; where $\vec{x}_0$ is a row vector of initial gains using the Z-N rule outcome on the original plant TF). Once the solution from the iterative process is found, pattern search could be used to examine the solution at the neighbourhood.

The (nominal system) result for the optimized PID is also shown on Table 1 and Table 2 (last column and row, respectively). It may seem slightly "inferior" in terms of PCT achieved compared to the F-R manual approach, however the optimized integer-order PID satisfies the level of $\|S(j\omega)\|_\infty$, robust stability bound and ride quality bound (due to the nature of the global optimization utilized). Overall the optimized PID offers a better solution, and is given by $K_{pid}^{opt.} = \dfrac{1.328s^2 + 2.533s + 44.84}{0.05548s^2 + 55.48s}$.

PID control.:		**Z-N**	**Z-N** detune	**Tyreus-Luyben**	**Tyreus-Luyben** (detune)	**F-R** manual	**Opt.** cstr.
P_{CT}	Stand. (% psg.)	76.19	65.15	92.16	64.50	63.12	64.83
P_{CT}	Seated (% psg.)	24.70	20.34	30.42	20.05	19.46	20.20
Stochastic (acceleration %g) @58m/s **							
R.Q.	Lateral accel. (%g)	2.709	2.936	2.719	3.042	3.110	3.031
R.Q.	Degrad.(%)	-4.884	3.095	-4.520	6.8	9.194	6.41

% psg. = % of passengers

TABLE 1. Performance assessment (P_{CT} / Ride quality (R.Q.)): PID conventional tuning approaches

PID rule	**GM(dB)**	**PM(deg)**	**B/W(rad/s)**	$\|S\|_\infty$
Z-N PID original	2.40	80.9	0.48	4.14
Z-N PID (detuned)	3.75	35.7	1	2.93
Tyreus-Luyben	2.83	96.89	0.08	3.6
Tyreus-Luyben (detune)	5.88	43.28	0.93	2.36
Freq.-Resp. (manual)	5.75	48.29	1	2.4
Optimized (constrained)	6.01	89.9	0.71	1.99

TABLE 2. Stability margins for the conventional PID controllers

5. **Fractional order control methods**

This section discusses the main contribution of this paper, in particular the impact of fractional order methods on advanced tilt control design. After a brief introduction of fractional calculus the design problem is approached in two ways: (i) design a Fractional order PID (FOPID) controller on the NMP TF, (ii) design an integer order PID controller on a shaped model of the plant TF via fractional order shaping filter cancelling portion of the TF's NMP zeros (the final controller comprises both the PID and shaping filter). Note that the analysis and design of fractional order controllers in MATLAB was performed via the *CRONE* toolbox [22].

5.1. **Fractional order calculus and control theory.** The birth date of Fractional order calculus relates to 1695 with a letter sent by L'Hospital to Leibniz on the topic of derivatives, which excited replies on the concept of 'non-integer' order i.e. a more generalized version of differentiation and/or integration. Various definitions for the general fractional differential/integral exist [30] (e.g. Riemann-Liouville definition, Caputo's definition etc.), with Caputo's approach offers the advantage of linking fractional order to physical realization and given by

$$ {}_a^C D_t^\alpha f(t) = \frac{1}{\Gamma(\alpha - n)} \int_a^t \frac{f^{(n)}(\tau)}{(t-\tau)^{\alpha+1-n}} d\tau, \tag{5.1} $$

where $(n-1 < \alpha < n)$ and $\Gamma(.)$ is the Gamma function. In addition, its Laplace transform is ([30])

$$ \int_0^\infty e^{-st} \left\{ {}_0^C D_t^\alpha f(t) \right\} dt = s^\alpha F(s) - \sum_{k=0}^{(n-1)} s^{\alpha-k-1} f^{(k)}(0), \tag{5.2} $$

where $F(s) = \mathcal{L}\{f(t)\}$, $(n-1 < \alpha \leq n)$ and s is the Laplace operator.

Undoubtedly fractional order calculus enables more flexible analysis and design on dynamical systems and controller solutions. It offers great benefits in the area of control theory, and Fractional order PID control illustrates such benefits very delicately. Fractional order control design has gained, especially recently, popularity in the control literature [26] and a number of control design cases can be seen related to industry applications [17] [3] [27] [9] [5]. The approach is quite straightforward, i.e. instead of the classical case of integer powers of s, fractional powers are utilized. Hence, additional flexibility in tuning controller parameters arise (note that the fractional controllers can be approximated by appropriate IOR functions and a number of techniques to achieve these approximations exist). There are four well known fractional order controllers: CRONE (Commande Robuste d'Ordre Non Entier) [22] [12], Fractional order PID (FOPID) (aka $PI^\lambda D^\mu$),

Fractional Order Lead-Lag compensator [18] , and Fractional Order Phase shaper [6]. The work presented here stems from utilizing an FOPID and also utilizing [15] which proposes an FOC method that reduces the effect of unstable poles and zeros within a feedback control design framework.

The impact of FOC on advanced PID tilt control is twofold: (i) via design of a fractional PID while maintaining the original NMP model, (ii) via design of an integer order PID + fractional order-based shaping filter partially cancelling the NMPZ characteristics of the original model. The designs are discussed in the sections below.

5.2. **Fractional PID controller .** Fractional order PID (FOPID) also identified as $PI^{\lambda}D^{\mu}$ introduces two extra fractional variables to tune i.e. the integral order (λ) and derivative order (μ). Hence, FOPID enables a refined shaping of the compensated open-loop in terms of gain/phase (but at the expense of tuning an extra two controller parameters). Its transfer function (with limited fractional derivative) is given by

$$K_{FOPID}(s) = k_p \left(1 + \frac{1}{\tau_i s^{\lambda}} + \frac{\tau_d s^{\mu}}{N^{-1} s^{\gamma} + 1}\right), \tag{5.3}$$

where $k_p, \tau_i, \tau_d \in \mathbb{R}^+$ and also $\lambda, \mu, \gamma \in \mathbb{R}^+$ ($\mathbb{R}^+$ the set of positive real numbers). It is normal to set $\gamma = \mu$ for bi-properness (and hence not necessary to tune this parameter in the design process). The parameter N is the derivative cut-off frequency similar to the case of integer order PID.

Introducing two extra tuning terms adds complexity, albeit advanced software tools (as mentioned previously) and available processing power nowadays offer a smooth way of designing. Ultimately FOPID control is possible to implement (e.g. via integer-order approximation) although its structure can be more complex compared to conventional PIDs. FOPID benefits a more flexible control design in terms of loop shaping [13] and, while similar to conventional PID, enables shaping closer to Bode's ideal transfer function. FOPID is not the panacea of all solutions as there may be cases where it does not offer better performance compared to conventional PID, e.g. issues of rejection of input disturbance to the plant [13].

Once the FOPID is tuned [25] an IOR approximation [35], [36] can be obtained. A popular technique is the *Oustaloup recursive method* (i.e. recursive approach of fractional terms approximation) [35]. In fact, the IOR approximation is key to making FOPID largely attractive to the practising control engineer i.e. a more direct way of "refined" PID design (i.e. injecting extra lead-lag networks), thus fine shaping the frequency response of the compensated open loop. The notion of frequency shaping is also met in conventional control methods such as Quantitative Feedback Theory [11].

Tuning the FOPID follows the same optimization process to the conventional PID, i.e. (4.1), with the optimization running on *all fractional*

order PID controllers. In addition to the tuning of the three gains, two extra tuning variables of fractional order are included (one for the integral and one for the derivative part). Regarding the order of the integral and derivative terms, bounds need to be set such that the optimization has a meaning (for example to avoid excessive integral or derivative action as these will offer no advantage to control design). A bound for the fractional order of the integral term between 0.5 and 2 as well as a bound for the derivative term between approx. 0 and 1.25 suffice.

Deterministic(as per given units)		**FOPID (IOR)**
Lateral accel.	RMS Deviation ($\%g$)	2.605
	Peak value ($\%g$)	10.873
Roll gyro.	RMS deviation(rad/s)	0.031
	Peak value (rad/s)	0.140
	Peak jerk level($\%g/s$)	6.652
P_{CT} related	Standing (% of passengers)	51.437
	Seated (% of passengers)	12.619
Stochastic (acceleration %g) @58m/s **		
**Ride quality of non-tilt. train if running @ high speed = 2.848%g		
Ride quality	Tilting train	3.061
	Degradation (%)	7.485
Performance Margins		
Freq. resp.	Gain margin (linear)	6.49
	Phase margin (deg)	30.45
	Bandwidth (rad/s)	1.02
	$\|S(j\omega)\|_\infty$	2.00
	$\|W_\delta(j\omega)T(j\omega)\|_\infty$	1.00

TABLE 3. FOPID controller performance (results on full order IOR approximation of the controller)

The tuned FOPID that satisfied the constraints and provided minimum PCT value was:

$$K_{FOPID} = 0.2217\left(1 + \frac{1}{0.0843s^{1.673}} + \frac{0.029s^{0.913}}{0.001s^{0.913}+1}\right). \tag{5.4}$$

For its rational order implementation, the Oustaloup (5th order per fractional term) recursive approximation is utilized,

$$H(s) = s^{\mu}, \quad \mu \in \mathbb{R}^{+}, \text{ approximated by}$$
$$\widehat{H}(s) = C \prod_{k=-M}^{M} \frac{1 + s/\omega_k}{1 + s/\omega'_k}, \tag{5.5}$$

where $C, M, \omega_k, \omega'_k$ are given by the approximation procedure in [35].

The direct integer-order controller approximation is 16th order, and Table 3 presents the results (on nominal plant). Note that reduced order controller approximation are presented in the robustness and results section.

5.3. **PID with fractional order loop shaping .** We present the design of an integer-order PID on the shaped tilt design TF (shaped by use of NMP zero partial cancellation fractional order filter). The process is rather straightforward, (i) shape the plant TF by cancellation fractional order filter Q_n^{-1}; (ii) design the integer-order PID controller on the shaped plant $G_{yu} \times Q_n^{-1}$; (iii) the final controller is $Q_n^{-1} \times K_{pid}^{i}$ and implemented on the original plant TF (normally via integer order approximation of the Q-filter (e.g. via Oustaloup's method) i.e. $\tilde{Q}_n^{-1}$). This is motivated by seminal work of Merrikh-Bayat in [15] on fractional order filters partially cancelling unstable zeros. Only partial cancellation is considered, and an example [15] for a single unstable zero is shown in (5.6) (n: integer; z_u: nmp zero freq.)

$$1 - s/z_u = 1 - (s/z_u)^{n/n} = \left[1 - \left(\frac{s}{z_u}\right)^{1/n}\right] \sum_{k=1}^{n} \left(\frac{s}{z_u}\right)^{(k-1)/n}. \tag{5.6}$$

Such cancellation approach enables refined shaping of the plant by a series of lead-lag networks in the frequency domain (after integer-order approximation), potentially improving performance margins. Also, cancellation for $n = 2$ results to 1/2 portion of the NMP zeros characteristic is cancelled, $n = 3$ to 2/3, $n = 4$ to 3/4 etc. This clearly shows the impact of fractional order methods from a loop-shaping viewpoint.

The optimization problem (4.1) is also followed for the design in this section, but the design TF is now shaped by Q_n^{-1}. The consideration for initial conditions is similar to Section 4.2 (but the initial tuning rule is applied to the shaped design TF). The fractional order shaping filters Q_n^{-1}

for increasing NMPZ partial cancellation i.e. $n = 2$ up to $n = 7$ are:

$$Q_{\{n=2\}} = 0.0752s + 0.592s^{0.5} + 1. \tag{5.7}$$

$$Q_{\{n=3\}} = 0.0318s^{1.33} + 0.156s + 0.586s^{0.67} + 0.874s^{0.33} + 1. \tag{5.8}$$

$$Q_{\{n=4\}} = 0.0206s^{1.5} + 0.0803s^{1.25} + 0.2376s + 0.632s^{0.75} + 0.867s^{0.5} \ldots + 1.068s^{0.25} + 1. \tag{5.9}$$

$$Q_{\{n=5\}} = 0.0159s^{1.6} + 0.0541s^{1.4} + 0.14s^{1.2} + 0.32s + 0.696s^{0.8} \ldots + 0.901s^{0.6} + 1.1s^{0.4} + 1.21s^{0.2} + 1. \tag{5.10}$$

$$Q_{\{n=6\}} = 0.0135s^{1.6667} + 0.048s^{1.5} + 0.098s^{1.3333} + 0.21s^{1.1667} + 0.41s \ldots + 0.77s^{0.8333} + 0.96s^{0.6667} + 1.15s^{0.5} + 1.3s^{0.3333} + 1.31s^{0.1667} + 1. \tag{5.11}$$

$$Q_{\{n=7\}} = 0.012s^{1.7143} + 0.035s^{1.5714} + 0.076s^{1.4286} + 0.15s^{1.2857} \ldots + 0.28s^{1.1429} + 0.49s + 0.85s^{0.8571} + 1.02s^{0.7143} + 1.2s^{0.5714} \ldots + 1.37s^{0.4286} + 1.46s^{0.286} + 1.4s^{0.1429} + 1. \tag{5.12}$$

The controller gains for the integer-order PID portion, from the optimization process on the FO shaped plant, are (time const. in sec):

on case n=0:	$k_p = 0.045$	$\tau_i = 0.056$	$\tau_d = 0.533$
on case n=2:	$k_p = 0.1057$	$\tau_i = 0.0568$	$\tau_d = 0.6743$
on case n=3:	$k_p = 0.2821$	$\tau_i = 0.0810$	$\tau_d = 0.5315$
on case n=4:	$k_p = 0.4782$	$\tau_i = 0.0839$	$\tau_d = 0.5401$
on case n=5:	$k_p = 0.7691$	$\tau_i = 0.0917$	$\tau_d = 0.5165$
on case n=6:	$k_p = 1.000$	$\tau_i = 0.083$	$\tau_d = 0.574$
on case n=7:	$k_p = 1.398$	$\tau_i = 0.088$	$\tau_d = 0.555$

Implementing the FO filter Q_n^{-1} within the final controller $\tilde{Q}_n^{-1} \times K_{pid}^i$ also utilizes a 5th order Oustaloup continuous-time (OCT) realization [35]. Note that the overall controller order comprises the order of the PID (2nd order) portion and the order of $\tilde{Q}_n^{-1}$ after minimal realization (per case n). Hence, once the fractional order portion is approximated as mentioned above, the integer order of the final controller ranges from order= 8 for $n = 2$ up to order= 33 for $n = 7$ (giving the largest controller order in this scenario).

Note that: (a) for $n = 0$ the results are the ones obtained for the optimized integer-order PID as there is no NMP zero portion cancellation; (b) a 5th order OCT approximation of the fractional power was sufficient; (c) we consider up to $n = 7$ NMPZ cancellation as after that value performance differences become less significant. Figure 3 presents the compensated open loop magnitude frequency plot for $G_{yu} \times (\tilde{Q}_n^{-1} K_{pid}^i)$ per case n.

PID + Q_n^{-1} filter		**0** cancel.	**1/2** cancel.	**2/3** cancel.	**3/4** cancel.
P_{CT}	Stand. (% of passg.)	64.83	59.257	56.883	55.487
P_{CT}	Seated (% of passg.)	20.20	17.586	16.245	15.462
Stochastic (acceleration %g) @58m/s **					
R.Q.	Lateral accel. (%g)	3.031	2.929	2.955	2.98
R.Q.	Degrad. (%)	6.41	2.847	3.766	4.64

PID + Q_n^{-1} filter		**4/5** cancel.	**5/6** cancel.	**6/7** cancel.
P_{CT}	Stand. (% of passg.)	54.542	54.195	53.87
P_{CT}	Seated (% of passg.)	14.941	14.648	14.43
Stochastic (acceleration %g) @58m/s **				
R.Q.	Lateral accel. (%g)	3.002	3.010	3.024
R.Q.	Degradation (%)	5.395	5.692	6.178

TABLE 4. Performance assessment (P_{CT} / Ride qual.) under different PID + FO partial cancellation filter degree

Final Controller	**GM(dB)**	**PM(deg)**	**B/W(rad/s)**	$\|S\|_\infty$
PID only (0 canc.)	6.01	89.9	0.7	1.99
PID with 1/2 canc.	6.171	70.939	0.83	1.99
PID with 2/3 canc.	6.305	61.547	0.88	1.99
PID with 3/4 canc.	6.479	55.278	0.91	1.99
PID with 4/5 canc.	6.567	51.883	0.93	1.99
PID with 5/6 canc.	6.582	47.931	0.96	1.99
PID with 6/7 canc.	6.63	46.34	0.96	1.99

TABLE 5. Stability margins for PID+Q_n^{-1} controller

5.4. **Order reduction of the IOR approximation of the Fractional order controller.** In this section all fractional order controllers are already in rational (integer) order form as discussed previously (i.e. via Oustaloup's method and minimal realization where necessary). This normally results to large size integer order controllers.

We illustrate that the large size rational order controller can be approximated by a low-order one still preserving the properties of the closed loop

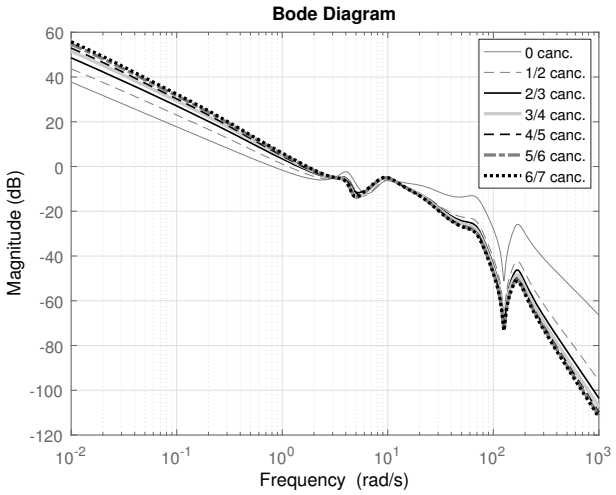

FIGURE 3. FO loop shaping: designed open loop magnitude plot

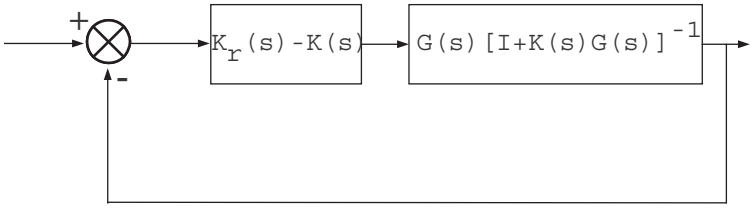

FIGURE 4. Feedback formulation for reduced-order controller design maintaining stability criteria

in which the controller would operate. Closed-loop controller reduction is utilized [20] with problem posed as a frequency-weighted one (Figure 4), i.e. emphasizing approximation in critical frequency ranges for the closed-loop system. Although there are other ways of controller reduction, the one used here is of particular interest to the control community in terms of maintaining closed-loop properties.

The process is as follows. A low-order controller $K_r(s)$, introduced in an additive sense, is required to replace the high-order IOR approximation of the FO controller, $K(s)$ in the closed-loop. This is shown in Figure 4 that characterizes the (most usual) frequency weighted formulation of the controller design. The reduction problem is to find (a stabilizing) low-order controller $K_r(s)$ such that the quantity (assuming only integer-order TFs)

$$||(K(j\omega) - K_r(j\omega))F(j\omega)||_\infty, \tag{5.13}$$

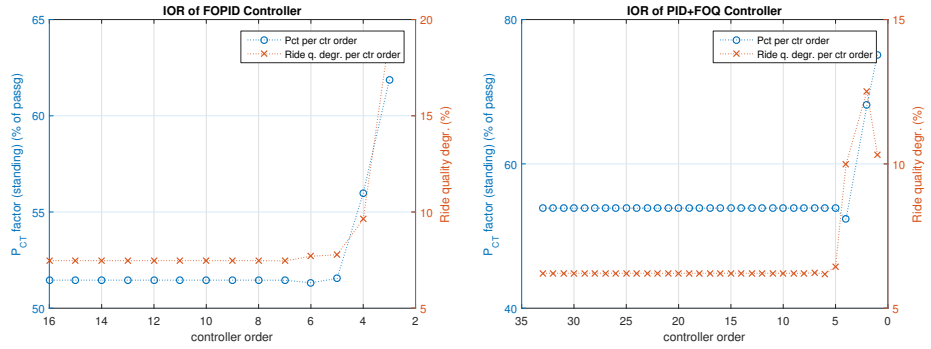

(a) Approximation of integer-order FOPID (b) Approximation of PID + $\tilde{Q}_{n=7}^{-1}$

FIGURE 5. Controller reduction and performance trade-off

is minimized, with $F(j\omega) = G(j\omega)(I+K(j\omega)G(j\omega))^{-1}$ (the reduction algorithm can be found in [20] and thus we omit its theoretical details). In the expressions $K(j\omega)$ and $G(j\omega)$ refer to the rational order approximation of the fractional order controllers and $G_{yu}(j\omega)$ resp. Note that there are also alternative frequency weighted formulations with more details also available in [20]. The frequency weight $F(j\omega)$ essentially introduces the importance of the true plant and controller information in the design procedure via the closed loop consideration. The low-order controller $K_r(s)$ will then be implemented on the original plant to control. Controller reduction could be incorporated as part of an extended global optimization problem, albeit normally designers investigate reduction after the full-order design[20].

Figure 5 presents (only the stable closed-loop cases) controller reduction level and the related PCT factor/ ride quality performance trade-off.

A 6th order controller for the approximated FOPID case and a 5th order for the approximated loop shaping controller maintain even the typical robustness properties of the closed-loop. This illustrates the usefulness of controller reduction in closed-loop (achieved 63% reduction for the approximated FOPID case, and 85% reduction for the loop-shaping one). Note that controller order has immense impact on hardware resources requirements for practical implementation, i.e. low-order controllers are always favourable (see example of FPGA-implemented LQG controllers in [8]).

6. **Results**

The discussion of the performance of the fractional-order based controllers is utilizing their integer-order (approximation) versions. When reduced order controller cases are used, this is denoted clearly on the relevant figures and tables and/or discussion lines. Due to limited space we

refer to the following reduced order controllers (when these are utilized in the discussion) as: (**CA**) the Optimized integer-order PID (Section (4.2)); (**CB**) *the 6th order reduced integer-order* approximation of the FOPID (Section 5.2); (**CC**) *the 5th order reduced integer-order* approximation of loop-shaped PID by $\tilde{Q}_{n=7}^{-1}$ (Section 5.3).

Also we present important vehicle parameters used [39]: $y_{\rm v}, y_b, y_0$ lateral displ. of body,bogie and railtrack (m); $\theta_{\rm v}, \theta_b, \theta_r$ roll displ. of body, bogie and airspring reservoir (rad); θ_0 rail track cant, curve radius (rad); $m_{\rm v}, i_{\rm vr}$ half body mass 19000(kg) and roll inertia 25000(kgm); m_b, i_{br} bogie mass 2500(kg) and roll inertia 1500(kgm^2); k_{az}, k_{sz} airspring area stiffness, $210e^3$ N/m and series stiffness, $620e^3$ N/m; k_{rz}, c_{rz} airspring reservoir stiffness, $244e^3$ N/m and damping, $33e^3$ Ns/m; k_{sy}, c_{sy} secondary lateral stiffness, $260e^3$ N/m and damping, $33e^3$ Ns/m; y_w bogie kinematics displ. (m).

6.1. **Nominal Performance (nominal plant and controllers).** Nominal system performance results have been presented in previous sections, while here a set of time–domain simulation figures is included to complement the design outcome.

Figure 6(b) illustrates the immense benefit of fractional order based control on improving tilt following (with full order control). Figure 6(c) and Figure 6(d) utilize reduced order controllers and further illustrate the benefit of fractional order based control in non-preview tilt, i.e. its close proximity to the industrial-norm curving response of tilt with precedence (tilt precedence schemes are more complex as described earlier). The precedence (preview) scheme uses tilt angle preview signals for 60% tilt compensation and integer-order PID for tilt following [40].

6.2. **Robust performance (plant uncertainty).** The perturbation characteristics of the plant are (see Figure 7): (i) **P1/P2** 20% body mass increase/decrease; (ii) **P3** 20% dynamic body mass decrease and 40%(20%) decrease (increase) in secondary vertical and roll suspension damping (stiffness); (iii) **P4** 20% dynamic body mass increase and 30%(20%) decrease (increase) in secondary vertical and roll suspension stiffness (damping). The rationale behind the parameter perturbation choice is: vehicle body mass variation serves as a mechanism to affect (vehicle dynamics) and NMPZ locations, while variation of the listed secondary suspension parameters will affect vehicle dynamics (not NMPZ locations).

Note that: (i) vehicle body mass variation affects NMP zero locations of the perturbed plant, (ii) vehicle body mass increase (P1 and P4) forces a 13% increase in the "slow" NMPZ frequency and a 25% decrease in the "faster" NMPZ frequency compared to the nominal plant P0, (iii) vehicle body mass decrease (P2 and P3) forces a 9% decrease in the "slow" NMPZ

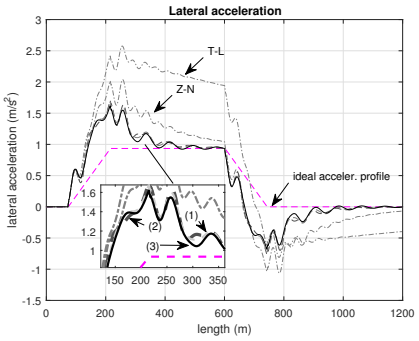

(a) 1- Z-N detuned, 2- T-L detuned, 3- F-R manual

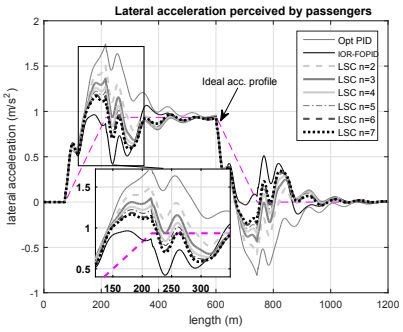

(b) Optim. PID, IOR-FOPID, PID+$\tilde{Q}_n^{-1}$ (LSC) for $n = 2, \ldots, 7$ (no reduction yet)

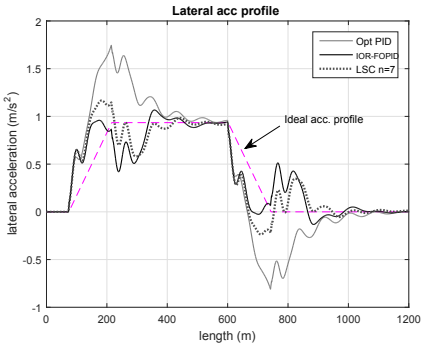

(c) Controllers: **(CA)**, **(CB)**, **(CC)**

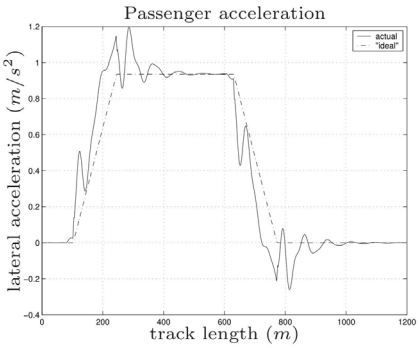

(d) Tilt preview (same vehicle setup)

FIGURE 6. Passenger acceleration (deterministic)

frequency and a 36% increase in the "faster" NMPZ frequency compared to case P0, (iv) varying secondary suspension (airpsring and roll) damping and/or stiffness does not affect the unstable zero locations as expected (note that only lateral suspension characteristics impact NMPZ locations).

The reduced order controllers maintain the required robust stability result, see Figure 8. This is further supported in Table 6 illustrating PCT and ride quality degradation for the different plants (noting that the controllers where designed on the nominal plant i.e. $P0$). Robust stability is clearly seen on PCT (as it directly treats deterministic problems), however the design naturally does not directly cater for robust ride quality performance (i.e. robust stochastic criterion, not considered here). Plant case $P4$ is a rather extreme case of uncertainty (e.g. under such conditions the vehicle would be retired for maintenance/replacement of the suspensions), but simply illustrates the extend of achieved robust stability.

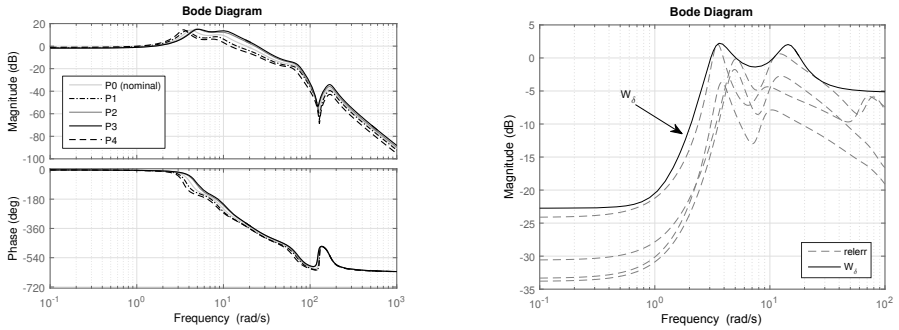

(a) Frequency response of P0-4 plants (b) Multiplicative uncertainty bound W_δ

FIGURE 7. Plant uncertainty (note in (b) W_δ is a 4th integer-order bound and 'relerr' denotes $|\frac{G_p(j\omega)}{G_{nom}(j\omega)} - 1|$)

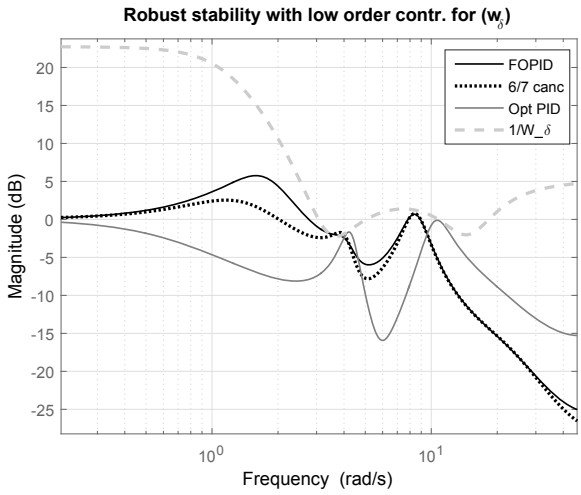

FIGURE 8. Closed loop robust stability: **(CA)**, **(CB)**, **(CC)**

7. **Conclusion**

A rigorous study on the impact of fractional order methods in design of PID-type tilt controllers was presented. The problem was posed in a straightforward single-input single-output control framework. The substantial impact of fractional order based methods on designing advanced tilt controllers compared to the integer-order conventional counterparts was illustrated. With the proposed solution there is no need for disturbance

Plant id	**IOR-FOPID 6th order (CB)**		**Loop-shaping 5th order (CC)**		**Optim. PID 2nd order (CA)**	
	P_{ct} (% of psg.)	**rqd** (%)	P_{ct} (% of psg.)	**rqd** (%)	P_{ct} (% of psg.)	**rqd** (%)
P0	51.32	7.70	53.84	6.45	64.83	6.41
P1	51.15	24.10	55.49	22.25	66.10	11.61
P2	53.30	-0.25	56.59	-1.47	66.00	12.19
P3	59.35	-1.17	62.69	-2.18	67.47	40.83
P4	52.75	89.77	56.82	89.20	70.12	24.96

TABLE 6. Robust performance results for **(CA)**, **(CB)**, **(CC)**

feed-forward hence avoid estimators. We emphasize the path from fractional order tuning to integer-order approximation and controller reduction while maintaining robust stability. The immense performance benefits were shown via simulation results on a comprehensive tilt vehicle model. With no loss of generality, the design framework in the paper can be the basis for other active suspension control design. Fractional order methods enable considerable opportunities in advanced control design for vehicle applications. A combined deterministic-stochastic robust control design on tightening tilting train ride quality performance while achieving curve following performance under uncertainty is investigated by the authors.

Acknowledgements

The first author acknowledges MARA Malaysia for supporting the studies under PhD scholarship ref. 330407137000. The authors would also like to thank the anonymous reviewers for their constructive comments, which helped us to further improve the quality of this manuscript.

References

[1] K.J. Åström, T. Hägglund, Advanced PID Control. **ISA** - *The Instrum., Systems, and Autom. Society*, Res. Triangle Park, NC (2006).

[2] A. Banos, J. Cervera, P. Lanusse, J. Sabatier, Bode optimal loop shaping with CRONE compensators. *Journal of Vibration and Control* **17**, No 13 (2011), 1964–1974.

[3] G.W. Bohannan, Analog fractional order controller in temperature and motor control applications. *Journal of Vibration and Control* **14**, No 9–10 (2008), 1487–1498.

[4] D. Boocock, B.L. King, The development of the prototype advanced passenger train. *Proc. of the Institution of Mechanical Engineers* **196**, No 1 (1982), 35–46.

[5] R. Caponetto, S. Graziani, V. Tomasello, A. Pisano, Identification and fractional super-twisting robust control of IPMC actuators. *Fract. Calc. Appl. Anal.* **18**, No 6 (2015), 1358–1378; DOI: 10.1515/fca-2015-0079; https://www.degruyter.com/view/j/fca.2015.18.issue-6/issue-files/fca.2015.18.issue-6.xml.

[6] Y. Chen, K.L. Moore, B.M. Vinagre, I. Podlubny, Robust PID controller autotuning with a phase shaper. In: *1st IFAC Workshop on Fractional Differentiation and its Applications 2004* (2004), 162–167.

[7] E.F. Colombo, E. Di Gialleonardo, A. Facchinetti, S. Bruni, Active carbody roll control in railway vehicles using hydraulic actuation. *Control Eng. Practice* **31** (2014), 24–34.

[8] K. Deliparaschos, K. Michail, A. Zolotas, S. Tzafestas, FPGA-based efficient hardware/software co-design for industrial systems with systematic sensor selection. *Journal of Elec. Eng.* **67**, No 3 (2016), 150–159.

[9] E. Gonzalez, L. Dorcak, C.A. Monje, J.Valsa, F. Caluyo, I. Petráš, Conceptual design of a selectable fractional-order differentiator for industrial applications. *Fract. Calc. Appl. Anal.* **17**, No 3 (2014), 697–716; DOI: 10.2478/s13540-014-0195-z; https://www.degruyter.com/view/j/fca.2014.17.issue-3/issue-files/fca.2014.17.issue-3.xml.

[10] F. Hassan, A.C. Zolotas, R. Margetts, Improved PID control for tilting trains. In: *Students on Applied Engineering (ISCAE), International Conference for IEEE* (2016), 269–274.

[11] I.M. Horowitz, *Quantitative Feedback Design Theory: (QFT)*, Vol. **1**. Boulder, Colo., QFT Publications (1993).

[12] A. Lamara, G. Colin, P. Lanusse, A. Charlet, D. Nelson-Gruel, Y. Chamaillard, Pollutant reduction of a turbocharged diesel engine using a decentralized MIMO CRONE controller. *Fract. Calc. Appl. Anal.* **18**, No 2 (2015), 307–332; DOI: 10.1515/fca-2015-0021; https://www.degruyter.com/view/j/fca.2015.18.issue-2/issue-files/fca.2015.18.issue-2.xml.

[13] P. Lanusse, J. Sabatier, and A. Oustaloup, Extension of PID to fractional orders controllers: a frequency-domain tutorial presentation. *IFAC Proceedings* **47**, No 3 (2014), 7436–7442.

[14] J.T. Machado, F. Mainardi, and V. Kiryakova, Fractional calculus: Quo Vadimus? (Where are we going?). *Fract. Calc. Appl. Anal.*, **18**, No 2 (2015), 201–218; DOI:10.1515/fca-2015-0031; https://www.degruyter.com/view/j/fca.2015.18.issue-2/issue-files/fca.2015.18.issue-2.xml.

[15] F. Merrikh-Bayat, Fractional-order unstable pole-zero cancellation in linear feedback systems. *J. of Proc. Control* **23**, No 6 (2013), 817–825.

[16] C.A. Monje, Y. Chen, B.M. Vinagre, D. Xue, V. Feliu-Batlle, *Fractional-order Systems and Controls: Fundamentals and Applications*. Springer Science & Business Media (2010).

[17] C.A. Monje, B.M. Vinagre, V. Feliu-Batlle, Y. Chen, Tuning and auto-tuning of fractional order controllers for industry applications. *Control Engineering Practice* **16**, No 7 (2008), 798–812.

[18] C.A. Monje, B.M. Vinagre, A.J. Calderón, V. Feliu-Batlle, Y. Chen, Auto-tuning of fractional lead-lag compensators. *IFAC Proceedings* **38**, No 1 (2005), 319–324.

[19] K. Moskvitch, The trouble with trying to make trains go faster. In: *BBC Future* (2014), http://www.bbc.com/future/story/20140813-the-challenge-to-make-trains-fast.

[20] G. Obinata, B.D.O. Anderson, *Model Reduction for Control System Design*. Springer Verlag, New York (2001).

[21] A. Orvnäs, On active secondary suspension in rail vehicles to improve ride comfort. *Doctoral Thesis*, KTH, Sweden (2011).

[22] A. Oustaloup, P. Melchior, P. Lanusse, O. Cois, F. Dancla, The CRONE toolbox for Matlab. In: *Computer-Aided Control System Design (CACSD 2000), IEEE International Symposium* (2000), 190–195.

[23] A. Oustaloup, Fractional order sinusoidal oscillators: optimization and their use in highly linear FM modulation. *IEEE Trans. on Circuits and Systems* **28**, No 10 (1981), 1007–1009.

[24] J.T. Pearson,, R.M. Goodall, I. Pratt, Control system studies of an active anti-roll bar tilt system for railway vehicles. *Proc. of the Institution of Mechanical Engineers, Part F: J. of Rail and Rapid Transit* **212**, No 1 (1998), 43–60.

[25] I. Petráš, Tuning and implementation methods for fractional-order controllers. *Fract. Calc. Appl. Anal.* **15**, No 2 (2012), 282–303; DOI: 10.2478/s13540-012-0021-4; https://www.degruyter.com/view/j/fca.2012.15.issue-2/issue-files/fca.2012.15.issue-2.xml.

[26] M.S. Tavazoei, Time response analysis of fractional-order control systems: A survey on recent results. *Fract. Calc. Appl. Anal.* **17**, No 2 (2014), 440–461; DOI: 10.2478/s13540-014-0179-z; https://www.degruyter.com/view/j/fca.2014.17.issue-2/issue-files/fca.2014.17.issue-2.xml.

[27] I. Petráš, B. Vinagre, Practical application of digital fractional-order controller to temperature control. *Acta Montanistica Slovaca* **7**, No 2 (2002), 131–137.

[28] I. Petráš, The fractional-order controllers: Methods for their synthesis and application. *arXiv Preprint Math/* **0004064** (2000).

[29] I. Podlubny, Fractional-order systems and PI$^{\lambda}$D^{mu}-controllers. *IEEE Transaction on Automatic Control* **44**, No 1 (1999), 208–214.
[30] I. Podlubny, *Fractional Differential Equations*. Academic Press, San Diego (1999).
[31] I.E. Pratt, Active suspension applied to railway trains. *PhD Dissertation*, Loughborough University of Technology (1996).
[32] S. Skogestad, I. Postlethwaite, *Multivariable Feedback Control: Analysis and Design*, **2**. Wiley, New York (2007).
[33] M.S. Tavazoei, M. Haeri, Chaos control via a simple fractional-order controller. *Physics Letters A* **372**, No 6 (2008), 798–807.
[34] R. Vilanova, A. Visioli, *PID Control in the Third Millennium*. Springer, London (2012).
[35] B.M. Vinagre, I. Podlubny, A. Hernandez, V. Feliu, Some approximations of fractional order operators used in control theory and applications. *Fract. Calc. Appl. Anal.* **3**, No 3 (2000), 231–248.
[36] D. Xue, C. Zhao, Y. Chen, A modified approximation method of fractional order system. In: *International Conference on Mechatronics and Automation, IEEE* (2006), 1043–1048.
[37] Z. Yang, J. Zhang, Z. Chen, B. Zhang, Semi-active control of high-speed trains based on fuzzy PID control. *Procedia Engineering* **15** (2011), 521–525.
[38] R. Zhou, A. Zolotas, R. Goodall, Integrated tilt with active lateral secondary suspension control for high speed railway vehicles. *Mechatronics* **21** (2011), 1108–1122.
[39] A.C. Zolotas, J. Wang, R.M. Goodall, Reduced-order robust tilt control design for high-speed railway vehicles. *Vehicle System Dynamics* **46**, No S1 (2008), 995–1011.
[40] A.C. Zolotas, R.M. Goodall, Advanced control strategies for tilting railway vehicles. *UKACC Internat. Conference on Control, University of Cambridge* (2000).

[1], [2] *School of Engineering, College of Science*
University of Lincoln, Lincoln, LN6 7TS, UK
e-mail: [1] *fhassan@lincoln.ac.uk*
e-mail: [2] *azolotas@lincoln.ac.uk* *Received: November 24, 2016*

Please cite to this paper as published in:

Fract. Calc. Appl. Anal., Vol. **20**, No 3 (2017), pp. xxx–xxx,
DOI: 10.1515/fca-2017-.....